Interpolymer complexes of poly(methacrylic acid) and poly(2-alkyl-2-oxazolines): pH-mediated assembly, quantum-chemical insights into hydrogen-bond structure, and iodine vapour sorption

Polymer 356 (2026) 130028

Contents lists available at ScienceDirect

Polymer

journal homepage: www.elsevier.com/locate/polymer

Interpolymer complexes of poly(methacrylic acid) and poly(2-alkyl-2-oxazolines): pH-mediated assembly, quantum-chemical insights into hydrogen-bond structure, and iodine vapour sorption

Danelya N. Makhayeva [a], Dilnaz A. Tolegenova [a], Adina M. Abiyeva [a], Galiya S. Irmukhametova [a], Grigoriy A. Mun [a], Ruslan Y. Smyslov [b], Yulia E. Gorshkova [c,d], Vlada E. Ivanova [e], Felix N. Tomilin [e], Vitaliy V. Khutoryanskiy [f,*]

[a] Faculty of Chemistry and Chemical Technology, Al-Farabi Kazakh National University, Al-Farabi ave. 71, Almaty, 050040, Kazakhstan
[b] Institute of Macromolecular Compounds—Branch of B.P. Konstantinov Petersburg Institute of Nuclear Physics—NRC "Kurchatov Institute", Saint-Petersburg, Russia
[c] Joint Institute for Nuclear Research, Dubna, Russia
[d] Institute of Physics, Kazan Federal University, Kazan, Russia
[e] Kirensky Institute of Physics, Krasnoyarsk Scientific Centre, Siberian Branch, Russian Academy of Sciences, Krasnoyarsk, 660036, Russia
[f] Reading School of Pharmacy, University of Reading, Whiteknights, PO Box 224, Reading, United Kingdom

ARTICLE INFO

Keywords:
Poly(2-alkyl-oxazolines)
Poly(methacrylic acid)
Interpolymer complexes
Hydrogen bond
Iodine
Iodophors

ABSTRACT

The pH-mediated assembly of hydrogen-bonded interpolymer complexes between poly(methacrylic acid) and poly(2-alkyl-2-oxazolines) was investigated in aqueous solutions. Critical pHs (pH_{crit}) of complexation were determined across a range of polymer concentrations. The pH_{crit} shifted to higher values with the formation of interpolymer complexes moving from poly(2-methyl-2-oxazoline) to poly(2-ethyl-2-oxazoline) and poly(2-*n*-propyl-2-oxazoline), reflecting changes in hydrophilic-hydrophobic balance. Geometry optimisation and electronic structure calculations of the hydrogen bonding in the interpolymer complexes were performed using the quantum-chemical DFTB method with 3ob-3-1 parameters and the Grimme D3(BJ) dispersion correction. These calculations revealed that the most energetically favourable hydrogen bond structure involves the carbonyl oxygen of poly(2-alkyl-2-oxazoline) forming a bond with the hydrogen of the protonated carboxylic group of poly(methacrylic acid). Infrared spectroscopy and thermal analyses of these interpolymer complexes in the solid state were performed and show the presence of interactions between the polymers. The sorption of iodine vapours by the interpolymer complexes, as well as by the individual polymers, was investigated. It was found that poly(methacrylic acid) exhibits poor iodine sorption, whereas poly(2-alkyl-2-oxazolines) demonstrate a strong affinity for iodine. Complexation with poly(methacrylic acid) significantly reduces the ability of poly(2-alkyl-2-oxazolines) to sorb iodine vapours.

1. Introduction

Water-soluble polymers possess a distinctive ability to form supramolecular structures – known as macromolecular complexes – when mixed with other complementary functional polymers or certain small molecules [1–3]. These self-assembly processes are typically driven by specific interactions such as electrostatic attraction, hydrogen bonding and hydrophobic effects. The resulting macromolecular complexes often exhibit properties markedly different from those of the individual components, unlocking a wide range of potential applications.

A distinctive class of these macromolecular complexes is the hydrogen-bonded interpolymer complexes (IPCs), which form through interactions between poly(carboxylic acids) and non-ionic, proton-accepting polymers [4,5]. IPCs can form in both aqueous and certain organic solvents. A key prerequisite for strong hydrogen bonding, and thus stable IPC formation, is the presence of a sufficient fraction of non-ionised (undissociated) carboxylic acid groups (–COOH) in the poly (carboxylic acid). In contrast, ionised carboxylate groups ($-COO^-$) cannot donate hydrogen bonds and are therefore much less effective in forming the specific hydrogen-bonded IPCs with proton-accepting

* Corresponding author.
E-mail address: v.khutoryanskiy@reading.ac.uk (V.V. Khutoryanskiy).

https://doi.org/10.1016/j.polymer.2026.130028
Received 23 December 2025; Received in revised form 26 March 2026; Accepted 10 April 2026
Available online 10 April 2026

groups of non-ionic polymers.

The strong dependence of hydrogen-bonded complexation on the dissociation state of the carboxylic acid groups (–COOH/–COO^-) of poly (carboxylic acids) imparts pH-responsiveness to IPCs [6–8]. These complexes are typically insoluble under acidic conditions, where they exist in a hydrophobic, aggregated state [9]. As the pH increases, they gradually swell and unfold, ultimately leading to dissociation and dissolution. This pH-responsive behaviour makes IPCs particularly attractive for pharmaceutical applications. Indeed, a wide range of such applications has been explored in the literature [10–14].

Another important factor contributing to the formation of hydrogen-bonded IPCs in aqueous solutions is hydrophobic effects. Hydrophobic moieties in both poly(carboxylic acid) and non-ionic polymer contribute additional stabilisation to the IPC. For example, poly(methacrylic acid) generally forms more stable complexes with non-ionic polymers than the less hydrophobic poly(acrylic acid) [15–18]. Hydrophobic effects are especially pronounced when the non-ionic polymer exhibits a lower solution critical temperature in aqueous solution, further promoting complex formation through enhanced hydrophobic interactions [19, 20].

Water-soluble poly(2-alkyl-2-oxazolines) are an emerging class of polymers valued for their non-toxic nature, tunable hydrophilicity, broad functional versatility and cost-effective synthesis [21–24]. Methyl-, ethyl- and n-propyl-derivatives (PMeOx, PetOx and PnPOx) of poly(2-alkyl-2-oxazolines) are fully soluble in water. These polymers have been applied in various biomedical fields, including the formulation of solid drug dispersions [25–27], hydrogels [28], electrospun fibres [29], nanoparticles [30–32] and polymeric films for drug delivery [33].

In addition to their biomedical relevance, water-soluble poly(2-alkyl-2-oxazolines) exhibit distinct thermal and physicochemical properties that strongly depend on the structure of the side chain. These polymers are generally amorphous, although the degree of crystallinity and thermal behaviour may vary with molecular weight and alkyl substituent length. For example, recent studies have demonstrated that polyoxazoline crystallinity significantly affects glass transition and mechanical properties [34], and that the nature of the alkyl side chain influences thermal transitions and self-assembly behaviour in both solution and bulk states [35]. The T_g of poly(2-alkyl-2-oxazolines) decreases with increasing side-chain hydrophobicity, and more hydrophobic derivatives may exhibit low critical solution temperature (LCST) behaviour in water. These properties govern chain mobility and interpolymer interactions in aqueous systems.

The ability of water-soluble poly(2-alkyl-2-oxazolines) to form complexes with polymeric acids in aqueous solutions offers significant potential for the development of pharmaceutical dosage forms, smart coatings, nanoparticles, microcapsules and functional films [36–39]. However, systematic studies on their complexation with acidic polymers – both in comparison to other non-ionic water-soluble polymers and among different poly(2-alkyl-2-oxazoline) derivatives – are currently lacking. Furthermore, the specific proton-accepting groups within poly (2-alkyl-2-oxazolines) responsible for hydrogen bonding with the undissociated carboxylic acid groups (–COOH) of poly(carboxylic acid) or tannic acid remain unclear. The nitrogen atom in the polymer backbone and the carbonyl in the side chain are potential hydrogen bond acceptors that could be involved in this hydrogen bonding.

Another important property of water-soluble poly(2-alkyl-2-oxazolines) is their potential ability to bind molecular iodine. We recently demonstrated this ability for poly(2-ethyl-2-oxazoline) in aqueous solutions, showing iodine-binding capacity comparable to that of poly(N-vinylpyrrolidone), a polymer traditionally used in antiseptic iodine formulations [40]. Complexation of iodine with water-soluble polymers is advantageous for enhancing its antimicrobial properties, improving chemical stability, and reducing irritation potential. Moreover, iodine adsorption serves as a sensitive molecular probe for evaluating the polarity, hydrophobic–hydrophilic balance, and accessibility of functional groups within polymer complexes. Thus, studying iodine sorption provides valuable insight into the microenvironmental structure and intermolecular interactions governing the behaviour of interpolymer complexes.

In our previous study [41], we investigated the formation of IPCs between poly(2-alkyl-2-oxazolines) and poly(methacrylic acid) (PMAA) in solutions using polarised luminescence relaxation and small-angle X-ray scattering (SAXS). We demonstrated that hydrophobic interactions, influenced by the side-chain length of poly (2-alkyl-2-oxazolines), play a crucial role in IPC formation in both aqueous and methanol environments. A marked increase in the relaxation times of luminescently labelled PMAA (from 80 to 680 ns) confirmed the formation of these complexes. Furthermore, SAXS analysis revealed that the IPCs exhibit supramolecular organisation resembling nanohydrogels, comprising compact hierarchical structures ranging from 40 to 10.7 nm in size.

This work systematically investigates the formation of IPCs between poly(methacrylic acid) and three structurally distinct poly(2-alkyl-2-oxazoline) derivatives (PEtOx, PMeOx, and PnPOx) across a wide pH range. The properties and compositions of these IPCs in the solid state were characterised using elemental analysis, infrared spectroscopy and thermal analysis techniques. The likely nature of hydrogen bonding within the IPCs was elucidated through quantum-chemical calculations. Additionally, the absorption of iodine vapours by the individual poly(2-alkyl-2-oxazolines), poly(methacrylic acid) and their IPCs in the solid state was examined.

2. Materials and methods

2.1. Materials

Poly(2-ethyl-2-oxazoline) (PEtOx, Mw ≈ 50 kDa, PDI 3–4) was purchased from Sigma-Aldrich (UK), and poly(methacrylic acid) (PMAA, Mw ≈ 100 kDa) was obtained from Polysciences (China). Poly (2-methyl-2-oxazoline) (PMeOx) and poly(2-*n*-propyl-2-oxazoline) (PnPOx) were synthesised according to the procedure described in Ref. [26]. The molecular characteristics of the polymers were evaluated by gel permeation chromatography (GPC) using a Viscotek system (Malvern Instruments, UK) equipped with a 270 dual detector and a VE 3580 refractive index (RI) detector. The system was calibrated using PolyCAL™ polyethylene oxide and dextran standards, and measurements were carried out at 30 °C using 0.1 M $NaNO_3$ aqueous solution as the eluent.

The mass-average molar mass of PEtOx determined by GPC was 64.4 kDa (Đ = 2.4), while that of PMeOx was 36.8 kDa (Đ = 1.6), which is consistent with the expected changes in molecular characteristics during the synthesis. GPC analysis of PnPOx under these conditions was not feasible due to its limited solubility in the aqueous 0.1 M $NaNO_3$ eluent and its pronounced thermosensitivity above approximately 24 °C, which leads to phase separation during the measurement. Although alternative GPC methods using organic eluents (e.g., DMF/LiBr) have been reported for poly(2-oxazoline)s, such conditions were not applicable in the present study due to the solubility limitations of the polymer and the experimental setup used. Additional characterisation data of the polymers, including ^{1}H NMR spectra, FTIR spectra, and GPC chromatograms, are provided in the Supporting Information (Figs. S1–S3, Table S1).

2.2. Determination of critical pH values

IPCs were prepared by mixing aqueous solutions of the individual starting polymers at concentrations of 0.002, 0.010, and 0.050 unit-mol/L in equimolar proportions. Polymer concentrations in this work are expressed in unit-mol/L, which refers to the molar concentration of repeating units (monomer units) rather than entire polymer chains. For example, poly(methacrylic acid) (PMAA) has the molar mass of a single repeating unit of 86 g/mol. The solution with a concentration of 1 unit-

mol/L corresponds to dissolving 86 g of PMAA (regardless of its overall molar mass) in 1 L of water. Likewise, a 0.002-unit mol/L solution of PMAA corresponds to 0.172 g of PMAA (i.e., 86 g/mol × 0.002 mol) dissolved in 1 L of water. These concentrations of polymer solutions were standardised across all methods described below.

Turbidimetric measurements were conducted using a Shimadzu UV-1901i UV spectrophotometer (Germany) at $\lambda = 400$ nm [42]. Measurements for PEtOx and PMeOx solution mixtures with PMAA were performed at 25 °C, while those for PnPOx were carried out at 18 °C to prevent phase separation due to the polymer's lower critical solution temperature (LCST). All measurements were performed in a 1 mm path length quartz cuvette, using deionised water as the reference. Absorbance was recorded after mixing the polymer solutions, followed by 30 s of stirring.

Viscosity measurements were performed using a microviscometer (Anton Paar) equipped with a 1.59 mm diameter capillary. Experiments were conducted at 25 °C for PEtOx and PMeOx solutions, and at 18 °C for PnPOx solutions to account for their LCST behaviour. The dynamic viscosity of the IPC solutions was recorded under these conditions.

Dynamic light scattering (DLS) experiments with interpolymer complexes in solution were performed at a scattering angle of $\theta = 90°$. Measurements were conducted at 25 °C using a NanoBrook 90 Plus instrument (Brookhaven, USA) for PEtOx and PMeOx solutions, and at 18 °C for PnPOx solutions to avoid phase separation above its LCST. Data analysis was carried out using BIC Particle Solutions software, including the calculation of number-weighted hydrodynamic diameter (Dh) distribution functions. The DLS measurements were conducted in accordance with the general principles described in ISO 22412:2017 (Particle size analysis — Dynamic light scattering).

The pH of the solutions was adjusted from 2.0 to 8.0 with 0.100 M HCl and 0.100 M NaOH and determined using a Metrohm 781 pH/Ion Meter.

The critical pH values were determined as the intersection point of two linear segments fitted to the experimental data before and after the inflexion observed on the turbidity-pH and viscosity-pH curves.

All experiments were performed in triplicate, and the results are reported as mean ± standard deviation.

2.3. Physicochemical methods used for the characterisation of interpolymer complexes

For physicochemical analysis, dry IPCs were prepared by mixing the original polymer solutions at a concentration of 0.050 unit-mol/L in an equimolar ratio at a pH below 3.5. The resulting IPC precipitates were filtered and washed twice with distilled water to neutralise the pH, followed by a second filtration. The collected precipitate was then dried in a vacuum oven until dry matter was obtained.

2.3.1. Fourier transform infrared spectroscopy (FTIR)

The IR spectra of KBr pellets of dried IPC and individual polymers were recorded using a PerkinElmer Spectrum 65 FTIR spectrometer (USA) in the wavenumber range of 4000–450 cm^{-1}.

2.3.2. Elemental analysis

Determination of nitrogen in IPC samples was performed using a Vario Micro Cube CHNS elemental analyser (Elementar-Straße, Langenselbold, Germany). The analysis is based on high-temperature catalytic combustion of the sample in an oxygen-rich environment at temperatures up to 1200 °C, converting all elements into their gaseous oxides (CO_2, H_2O, SO_2, NO_x). The resulting gases were passed through oxidation and reduction columns, where NO_x was reduced to N_2, which was then separated from other gases using adsorption columns. Nitrogen was detected using a thermal conductivity detector, and its content was calculated based on the area under the N_2 peak.

2.3.3. Thermal analysis

The polymers and interpolymer complexes were thermally analysed using a SKZ1053A thermogravimetric analyser (China) at a heating rate of 5 °C/min in a dry nitrogen atmosphere (99.99% purity, flow rate 100 mL/min) using ceramic crucibles. The sample mass for both polymers and IPCs was approximately 10–12 mg.

Differential scanning calorimetry (DSC) experiments were carried out in the 30–300 °C temperature range using a SKZ1052 DSC instrument (China) in an air atmosphere, with a heating rate of 10 °C/min and a sample weight of 10 mg. Data were analysed using the 2023051113_s DSC Thermal Analysis software. Tzero™ aluminium pans were used for all calorimetric measurements, with an empty pan as the reference, and the mass of both the reference and sample pans was considered.

Since the *glass transition temperature (T_g)* is sensitive to moisture content, the samples were pre-dried in a drying oven at 80 °C for 48 h. Before measurements, the samples were additionally preheated to 100 °C on the instrument to ensure the removal of residual moisture. The DSC experiments were performed in a heat–cool–heat mode; however, due to instrumental limitations, the cooling scan could not be recorded, although controlled cooling was carried out between the heating cycles. The second heating scan was used for data interpretation.

2.4. Quantum-chemical calculations

Geometry optimisation and electronic structure calculations were performed using the quantum-chemical DFTB method with 3ob-3-1 parameters and the Grimme D3(BJ) dispersion correction [43]. To account for the solvent (ethanol), the SMD solvation model, which is based on the electron density of the solute and a continuum solvent model, was applied [44]. Infrared spectra were obtained by performing a Hessian calculation in vacuum (GF conditions) with Lorentzian broadening of 30. All calculations were carried out using the GAMESS software package [45].

2.5. Absorption of iodine vapours by the powders of the individual polymers and their interpolymer complexes

Iodine vapour sorption was investigated using the sublimation method as described previously in Ref. [46]. For this purpose, 10 mg samples of the dry polymers (PMAA, PMeOx, PEtOx, and PnPOx) and the corresponding interpolymer complexes (PMeOx–PMAA, PEtOx–PMAA, and PnPOx–PMAA) were used. Prior to the experiment, the samples were dried in a vacuum oven in order to minimise the influence of residual moisture. All samples were analysed in the form of finely dispersed dry powders and were placed on watch glasses inside a sealed desiccator containing 500 mg of crystalline iodine at the bottom. No direct contact between the iodine and the polymer samples was allowed. The desiccator was maintained in a water bath at 50 °C for 48 h to allow iodine vapour exposure. Preliminary experiments indicated that iodine uptake reached a plateau under these conditions, suggesting that the selected exposure time was sufficient to approach sorption equilibrium.

After exposure, the samples were removed from the desiccator and weighed specimens (2 mg) of the iodine-containing materials were dissolved in ethanol. The iodine concentration in the resulting solutions was determined spectrophotometrically using a Shimadzu UV-1901i spectrophotometer at 444 nm. All measurements were performed in triplicate and the results are reported as mean values ± standard deviation. The iodine concentration was calculated using a calibration curve constructed in the 0–0.1 mg/mL concentration range (Fig. S4, Supporting Information).

3. Results and discussion

3.1. Studies of the complexation in aqueous solutions

In aqueous solutions, the presence of undissociated carboxylic acid

groups (–COOH) in poly(carboxylic acids) is typically achieved by lowering the pH. As a result, most hydrogen-bonded IPCs form at pH values below a specific threshold known as the critical pH of complexation (pH_{crit}). The pH_{crit} depends on several factors, including the chemical nature of both polymers, their concentration and the presence of small molecules or inorganic ions in the solution [47]. This parameter has been proposed as a useful criterion for evaluating the ability of polymers to form hydrogen-bonded complexes: higher pH_{crit} values

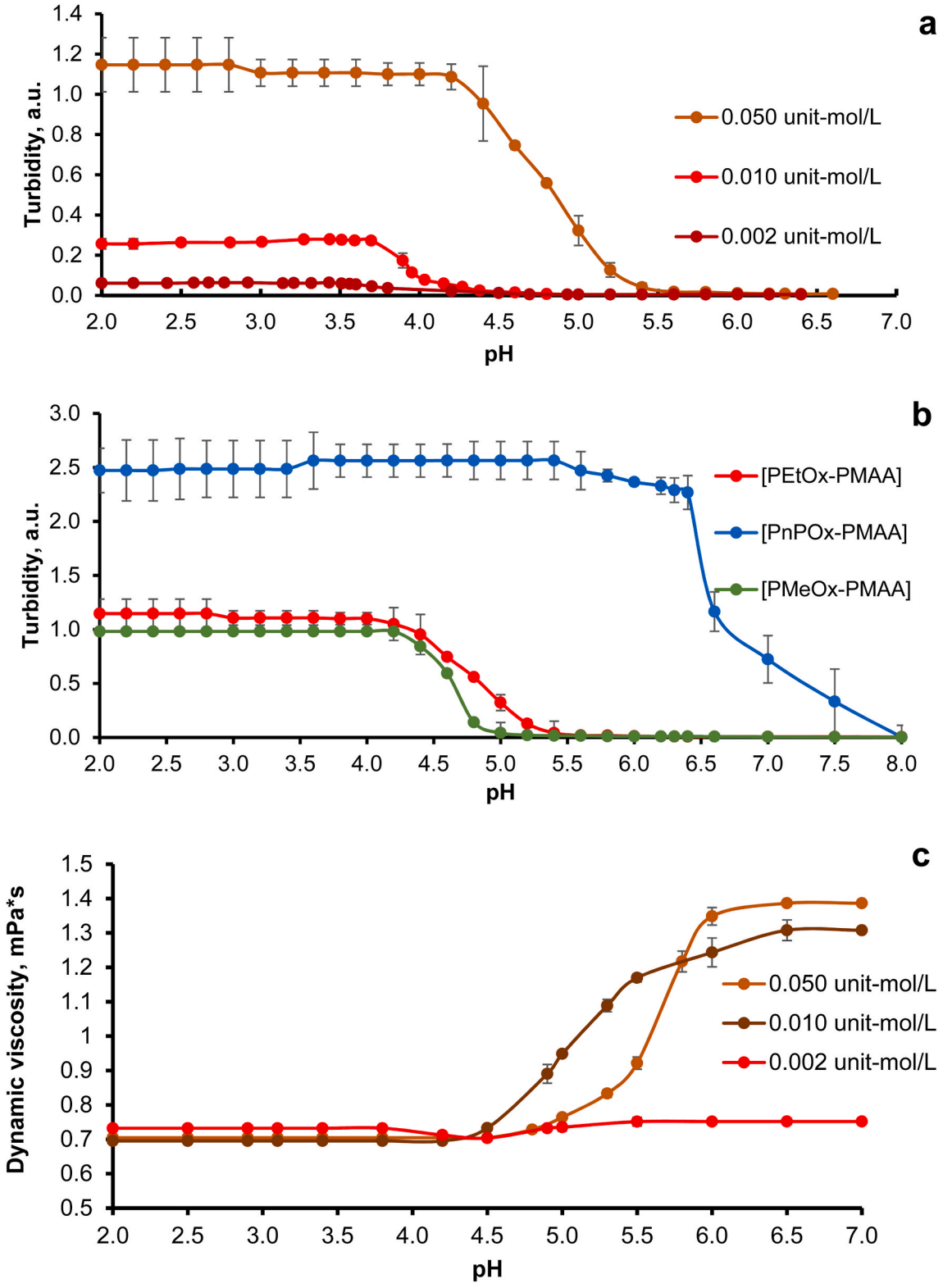

Fig. 1. pH-Responsive behaviour of PMAA–poly(2-oxazoline) complexes. (a) Turbidity–pH profiles of PMAA with PEtOx at different concentrations (0.002, 0.010, and 0.050 unit-mol/L);
(b) Turbidity–pH profiles of PMAA with PMeOx, PEtOx, and PnPOx at 0.050 unit-mol/L;
(c) Changes in the dynamic viscosity of PEtOx–PMAA solutions as a function of pH at different concentrations (0.002, 0.010, and 0.050 unit-mol/L).

indicate a stronger ability for IPC formation [48].

To determine the pH_{crit} values, aqueous solutions of PMAA with PMeOx, PEtOx, and PnPOx at concentrations of 0.050 unit-mol/L, 0.010 unit-mol/L, and 0.002 unit-mol/L, respectively, were mixed in a 1:1 M ratio. Turbidity was measured after mixing aqueous solutions of PMAA with PAOx at concentrations of 0.050 unit-mol/L and 0.010 unit-mol/L. Solutions at 0.002 unit-mol/L were initially transparent, and opacity appeared after decreasing the pH. Importantly, in control experiments, the individual polymers (PMAA, PMeOx, PEtOx, and PnPOx) did not exhibit any increase in turbidity upon pH reduction under the same conditions (Fig. S5, Supplementary Information). The formation of IPCs between PMAA and PMeOx, PEtOx, or PnPOx occurs below specific critical pH values. The effect of polymer concentration on these values was analysed, as shown in Fig. 1a, which presents the turbidity behaviour of PEtOx -PMAA mixtures across different pH levels: the pH_{crit} values were 5.2 for 0.050 unit-mol/L, 4.2 for 0.010 unit-mol/L, and 3.8 for 0.002 unit-mol/L. Turbidimetric curves for PMeOx -PMAA and PnPOx -PMAA are presented in Fig. S6, where a similar dependence of pH_{crit} on polymer concentration is observed. A distinct increase in turbidity over a narrow pH range marks the onset of interpolymer complex formation. Below this point, compact IPC particles are formed in solution and may further aggregate, leading to increased turbidity and, at sufficiently high concentrations, to precipitation. The data indicate that increasing the polymer concentration shifts the pH_{crit} toward higher values, which may be related to reduced ionisation of PMAA and enhanced intermolecular association at higher polymer content. It should be noted that the initial turbidity increase corresponds to the formation of primary interpolymer complex particles, whereas further turbidity growth at lower pH values may additionally involve aggregation of these particles. Control experiments performed for the individual homopolymers show no sharp turbidity transitions within the studied pH range, confirming that the turbidity increase observed in the mixtures originates from interpolymer complex formation rather than from phase separation of the individual polymers.

In the series of IPCs formed by PMeOx, PEtOx, and PnPOx with PMAA, the critical pH values increased from 4.8 for PMeOx, 5.2 for PEtOx and 7.5 for PnPOx (Fig. 1b), which correlates with the structural differences and the increasing hydrophobicity of these polymers. Greater hydrophobicity of the interacting PAOx enhances the stability of hydrogen-bonded interpolymer complexes by introducing additional hydrophobic interactions. The importance of this effect is demonstrated by the fact that polymers with more hydrophobic substituent groups form IPCs at higher pH_{crit} values, suggesting that complexation can occur under less acidic conditions. Similar trends have been observed in other IPC-forming systems. For example, Mun et al. [20] reported complex formation between copolymers of vinyl butyl ether (VBE) and vinyl ether of ethylene glycol with poly(acrylic acid), and found that increasing the content of the more hydrophobic VBE resulted in higher pH_{crit} values.

Complexation between polymers in solution is typically accompanied by conformational rearrangements of the macromolecular chains, leading to their compaction and a reduction in the hydrodynamic volume of polymer coils, which may result in a decrease in solution viscosity. Accordingly, dynamic viscosity can serve as an additional macroscopic indicator of interpolymer interactions in solution. As observed for turbidity measurements, the interaction between PEtOx and PMAA leads to a noticeable decrease in viscosity when the pH approaches the critical pH of complex formation (Fig. 1c). At pH values above pH_{crit}, the viscosity of the PEtOx/PMAA mixtures remains relatively high, reflecting the extended conformation of the polymer chains, whereas at lower pH, hydrogen-bond interactions between PMAA and poly(2-oxazoline)s induce chain compaction and the formation of interpolymer complex particles. It should be noted that complex formation and aggregation of IPC particles are distinct processes: at low concentrations (e.g., 0.002 unit-mol/L) the primary IPC particles remain dispersed and therefore produce only minor changes in viscosity, whereas at higher concentrations interparticle association becomes more pronounced. A similar trend is observed for complexes formed by PMeOx and PnPOx with PMAA (Fig. S7).

DLS is a valuable technique for characterising interpolymer complexes, providing insights into their particle size, distribution, and aggregation behaviour in solutions. It enables researchers to monitor size changes and evaluate the stability and formation of these complexes under varying conditions, such as pH, temperature, and ionic strength [49]. In this study, DLS was employed to characterise the size of IPC particles formed at varying pH levels. Fig. 2 presents the particle size distributions of IPCs formed between PEtOx and PMAA at various pH values, along with the corresponding mean diameters. These measurements were obtained at a low polymer concentration (0.002 unit-mol/L) as a representative example. Size distributions for additional IPC systems are provided in Fig. S8 (Supporting Information). The inset in Fig. 2 illustrates the variation in mean particle diameter of IPCs formed by PMAA with three different poly(2-oxazolines) as a function of pH. In all three systems, a marked increase in particle size was observed with decreasing pH, indicating the formation of primary interpolymer complex particles. Importantly, the pH range over which this increase occurs broadly aligns with the critical pH values determined by turbidimetric and viscometric analyses.

To provide additional information on the solution behaviour of the individual polymers, DLS size distributions of PMeOx, PEtOx and PnPOx were measured under the same conditions as those used for IPC formation (Fig. S9). The number-weighted distributions indicate that the polymers predominantly exist as individual macromolecules in aqueous solutions. The corresponding intensity-weighted distributions show larger apparent sizes due to the strong dependence of scattered light intensity on particle diameter (d^6). Importantly, the characteristic sizes observed for the individual polymers are significantly smaller than those detected for the interpolymer complexes, confirming that the larger particles observed in the mixtures originate from IPC formation rather than from aggregation of the individual polymers.

In all three systems, a pronounced increase in hydrodynamic diameter is observed upon decreasing pH. The onset of this size growth broadly coincides with the critical pH values determined from turbidimetric and viscometric measurements, supporting the formation of hydrogen-bond-driven interpolymer complexes in solution. Number-weighted size distributions indicate that the primary IPC particles grow gradually from approximately 8–12 nm at neutral pH to 30–50 nm in the complexation region.

Importantly, number-weighted and intensity-weighted distributions provide complementary information. While the number distributions reflect the size of the predominant IPC particles, intensity-weighted data reveal the presence of larger species at lower pH values. The appearance of particles in the several-hundred-nanometre range in intensity plots is attributed to secondary aggregation of preformed IPC particles rather than to the primary complexation event itself. Thus, interpolymer complex formation and subsequent aggregation represent distinct but consecutive processes: hydrogen bonding between complementary functional groups leads to the formation of primary IPC particles, whereas further size growth under more acidic conditions arises from interparticle association driven by reduced hydration and increased hydrophobic interactions.

A systematic dependence on the structure of the poly(2-alkyl-2-oxazoline) is evident. With increasing hydrophobicity of the side chain (PMeOx < PEtOx < PnPOx), larger hydrodynamic diameters and a more pronounced tendency toward aggregation are observed. This behaviour suggests that hydrophobicity primarily influences the aggregation propensity of IPC particles in aqueous media, while the initial hydrogen-bond-mediated complex formation occurs within a comparable nanoscale size range for all three polymers.

Subsequent DLS measurements were performed at a higher polymer concentration (0.050 unit-mol/L), revealing a substantial increase in IPC particle size and clearly indicating the formation of supramolecular

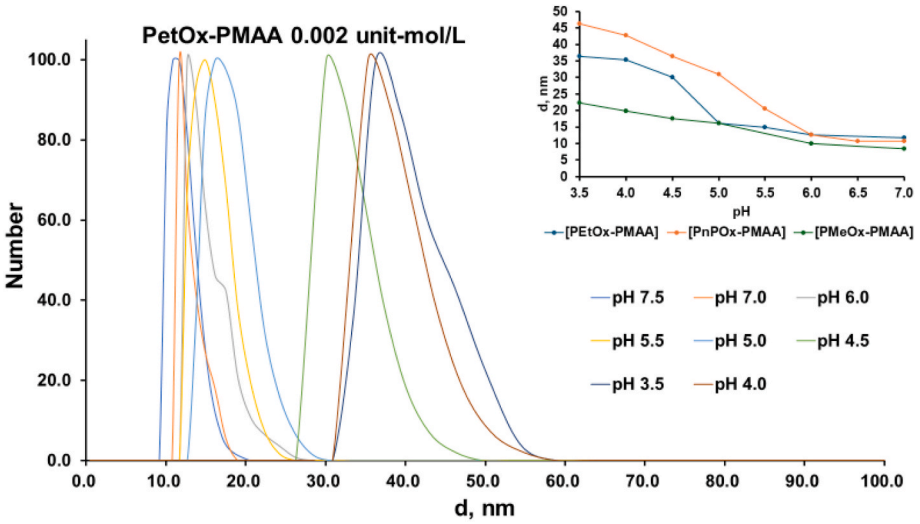

Fig. 2. Particle size distribution for PEtOx -PMAA complexes prepared at different pHs at polymer concentrations of 0.002 unit-mol/L. The inset shows the dependence of the IPCs hydrodynamic diameter on pH.

structures (Fig. 3). Consistent with turbidimetric and viscometric analyses, IPCs formed at pH values below the critical pH of complexation, which varied depending on the specific poly(2-oxazoline) used. Poly(2-oxazolines) containing more hydrophobic moieties exhibited higher pH_{crit} values, highlighting the role of hydrophobic interactions in stabilising IPCs. Minor deviations of several data points from the general trend are observed below pH_{crit}, which can be attributed to aggregation of particles and their poor colloidal stability. Notably, the observed pH_{crit} values are characteristic of strongly complexing nonionic polymers, such as poly(N-vinylpyrrolidone), poly(vinyl methyl ether) and poly(N-isopropylacrylamide), as reported in our previous studies [47, 50–52]. The inset in Fig. 3 illustrates the visual changes in the PnPOx -PMAA complex solution at various pH values. The solution transitions from completely transparent at pH 7.5 to turbid at pH 6.5, and to a partially flocculated system at pH 5.5. These observations further support the strong ability of this system to form IPCs, likely driven by a combination of hydrogen bonding and hydrophobic interactions.

3.2. Studies of IPCs in solid state

The IPCs prepared by mixing 0.050 unit-mol/L aqueous solutions of PMAA with different poly(2-oxazolines) at pH < 3.5 were isolated by centrifugation, the precipitates were washed with deionised water and dried. These samples were used to study their properties in the solid state.

Fig. 4 shows the FTIR spectra of PMAA, PEtOx, and their IPC. The characteristic absorption bands of pure PMAA are observed at approximately 1708 cm^{-1} (C═O stretching vibration of the carboxylic group) and 1181 cm^{-1} (C–O stretching vibration). The band at 1486 cm^{-1} corresponds to C–H bending vibrations of the polymer backbone. The FTIR spectrum of pure PEtOx exhibits a characteristic amide carbonyl stretching band at 1643 cm^{-1}, along with a broad absorption band in the

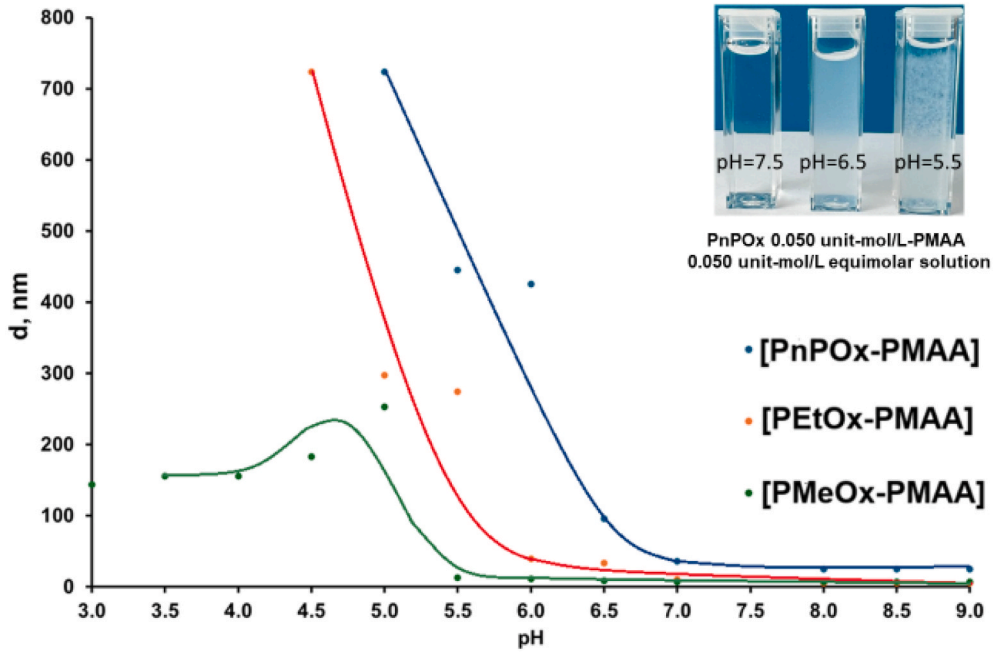

Fig. 3. Variation in particle size of PnPOx -PMAA, PEtOx -PMAA, and PMeOx -PMAA as a function of pH, with both polymers used at concentrations of 0.050 unit-mol/L. The inset shows the photographs of PnPOx -PMAA solutions at pH 7.5, 6.5, and 5.5. Trendlines are included for visual guidance.

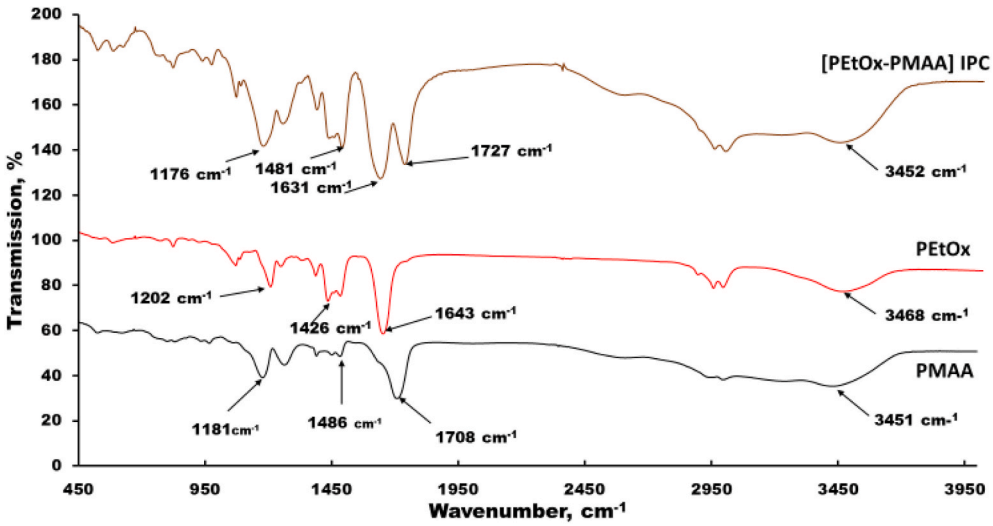

Fig. 4. FTIR spectra of PMAA, PEtOx and their IPC.

3300–3700 cm^{-1} region attributed to O–H stretching vibrations of bound water, indicating partial hydration. The characteristic C–H backbone vibration is observed at 1426 cm^{-1}. In the spectrum of the IPC, noticeable changes occur in the carbonyl stretching region. Upon complex formation, the PMAA carbonyl band shifts from 1708 cm^{-1} to 1727 cm^{-1} ($\Delta\nu = 19$ cm^{-1}), while the C═O band of PEtOx shifts from 1643 cm^{-1} to 1631 cm^{-1} ($\Delta\nu = 12$ cm^{-1}). These spectral changes suggest a redistribution of hydrogen-bonding interactions between the carboxylic groups of PMAA and the amide carbonyl groups of PEtOx. Additional variations in band intensity and position within the 1200–1700 cm^{-1} region (including the band at 1176 cm^{-1}) are consistent with intermolecular interactions in the interpolymer complex.

Similar spectral features are observed for the [PMeOx–PMAA] and [PnPOx–PMAA] interpolymer complexes (Fig. S10). In both systems, noticeable changes occur in the carbonyl stretching region upon complex formation. For the [PMeOx–PMAA] IPC, the PMAA carbonyl band at 1708 cm^{-1} shifts to 1734 cm^{-1}, while the C═O band of PMeOx at 1636 cm^{-1} shifts to 1638 cm^{-1}.

In the case of the [PnPOx–PMAA] complex, the PMAA carbonyl band shifts from 1708 cm^{-1} to 1728 cm^{-1}, accompanied by a slight shift of the PnPOx amide carbonyl band from 1644 cm^{-1} to 1637 cm^{-1}. In both systems, additional variations in band intensity and peak shape are observed in the 1200–1700 cm^{-1} region, further indicating modifications in the hydrogen-bonding network upon interpolymer complex formation. These results are consistent with those obtained for the PEtOx–PMAA system and confirm the general nature of the intermolecular interactions in PAOx–PMAA complexes.

These spectral changes are consistent with previous reports for similar IPCs. For example, Lichkus et al. [53] and Matsuda et al. [54] reported that the FTIR spectra of the IPCs formed between PEtOx and PMAA in solutions differed notably from simple polymer blends, with the former showing sharper and more defined peaks, indicating ordered hydrogen-bonded structures. In our study, similar effects were observed not only for PEtOx –PMAA complexes but also for PMeOx –PMAA and PnPOx –PMAA complexes (Fig. S10). In all systems, the characteristic carbonyl stretches of PMAA (1708 cm^{-1}) consistently shift to higher wavenumbers, while C═O stretching bands of PAOx broaden and broaden and shift to lower wavenumbers, confirming hydrogen bond formation. The C–N stretching region (1200–1500 cm^{-1}) also undergoes noticeable changes in the intensity and position, supporting the presence of hydrogen bonding.

The properties of the IPCs in the solid state were investigated using elemental and thermal analysis. The results presented in Table 1 show the nitrogen content of the individual polymers and their IPCs together with selected thermal characteristics of these materials. The highest nitrogen content was observed for PMeOx (15.93 ± 0.13%), which is close to its theoretical value of 16.46%, followed by PEtOx (14.01 ± 0.07% vs. 14.13%) and PnPOx (11.68 ± 0.11% vs. 12.38%), reflecting structural differences between the polymers. The small discrepancies between experimental and theoretical values may be attributed to the presence of residual moisture in the polymer samples.

Upon complexation with nitrogen-free PMAA, a significant decrease in nitrogen content was observed for all IPCs (6.06–6.92%), reflecting the incorporation of PMAA into the complex structure. In particular, the nitrogen contents were 6.42 ± 0.03% for IPC [PMeOx–PMAA], 6.92 ± 0.17% for IPC [PEtOx–PMAA], and 6.06 ± 0.17% for IPC [PnPOx–PMAA]. Based on these values, the approximate molar ratios of the components in the IPCs were estimated as 1:1.27 for [PMeOx]:[PMAA], 1:1.10 for [PEtOx]:[PMAA], and 1:1.15 for [PnPOx]:[PMAA]. The slight deviations from the ideal 1:1 stoichiometric ratio can be attributed to the presence of residual bound water and the inherent limitations of elemental analysis for hygroscopic polymer systems. Nevertheless, the

Table 1
Results of elemental and thermal analysis of individual polymers and their IPCs.

Sample	N, %	Composition of IPC [PaOx]:[PMAA]	Water content in the samples, %	T (onset of degradation), °C[a]	T_g, °C[b]
PMAA	-	-	0.73	213	226
PMeOx	15.93 ± 0.13	-	16.65	367	80
PEtOx	14.01 ± 0.07	-	4.87	387	61
PnPOx	11.68 ± 0.11	-	1.83	383	42
IPC [PMeOx-PMAA]	6.42 ± 0.03	1:1.3	3.09	180	105
IPC [PEtOx-PMAA]	6.92 ± 0.17	1:1.1	1.83	220	117
IPC [PnPOx-PMAA]	6.06 ± 0.17	1:1.2	3.95	305	114

[a] Determined by the TGA method.
[b] Determined by the DSC method.

obtained compositions are consistent with a model in which hydrogen bonding occurs predominantly between the carboxylic groups of PMAA and the amide groups of poly(2-oxazolines), leading to interpolymer complexes with compositions close to equimolar.

TGA was employed to investigate the thermal properties of the samples, with the resulting thermograms shown in Fig. 5. An initial weight loss was observed in all samples between 25 and 100 °C, typically attributed to the evaporation of residual water. The calculated water contents are summarised in Table 1. All three poly(2-oxazoline) samples exhibited higher water content compared to PMAA, reflecting their pronounced hydrophilicity. A clear correlation was observed between water content and polymer structure: the most hydrophilic polymer, PMeOx, contained 16.65% water, followed by PEtOx with 4.87%, and PnPOx with 1.83% - values consistent with their respective chemical compositions. The IPC samples were expected to exhibit slightly lower residual water content compared to the individual polymers, which was indeed observed for the PMeOx –PMAA and PEtOx–PMAA complexes. This reduction is likely due to increased hydrophobicity and hydrogen-bond-mediated sequestration of hydrophilic groups. However, the PnPOx–PMAA complex displayed a slightly higher residual water content than the individual polymers. This could potentially be related to less efficient packing or weaker hydrogen bonding interactions within this particular complex, leading to greater retention of loosely bound water. It is also possible that steric hindrance from the bulkier side chains of PnPOx reduces the extent of complexation with PMAA, resulting in a more open structure capable of retaining moisture. Alternatively, differences in residual water content may reflect variations in the drying efficiency of individual samples or experimental variability. Each TGA measurement was performed only once, and therefore, the observed difference may not be statistically significant. Further replicate experiments would be required to confirm the reproducibility of this observation.

Following the loss of residual water, all polymers and their interpolymer complexes undergo thermal degradation upon heating, with the specific degradation temperatures depending on the chemical structure of each material. PMAA exhibits two distinct degradation stages, with onsets at approximately 195 °C and 375 °C. The initial degradation stage is likely associated with an anhydridisation reaction, while the subsequent stage corresponds to degradation of the polymer backbone. This thermal degradation profile is consistent with previously reported data [55]. All poly(2-oxazolines) exhibited a single-stage thermal degradation, with onset temperatures varying depending on the polymer structure. PEtOx and PnPOx showed similar degradation onset temperatures at 387 °C and 383 °C, respectively, indicating greater thermal stability compared to PMeOx, which began to degrade at approximately 367 °C. According to the literature [34,56], both PMeOx and PnPOx exhibit thermal stability up to approximately 300 °C, with significant weight loss occurring between 300 and 400 °C, indicating degradation of the polymer backbone, while only a small amount of carbonaceous residue remains above 600 °C. The degradation profiles of the IPCs differed from those of the individual polymers. The PMeOx –PMAA complex exhibited enhanced thermal stability compared to PMeOx alone but remained less stable than PMAA. In contrast, the PEtOx–PMAA and PnPOx –PMAA complexes showed reduced thermal stability relative to their respective individual polymers.

DSC was employed to investigate the thermal behaviour of the individual polymers and their IPCs, with particular emphasis on determining their glass transition temperatures (T_g). To eliminate the influence of thermal history and residual moisture redistribution, the second heating scan was used for the analysis. The T_g values obtained for the individual poly(2-oxazolines) were consistent with literature data [57–59], with transitions observed at approximately 80 °C for PMeOx, 61 °C for PEtOx, and 42 °C for PnPOx (Fig. 6A). For PMAA, literature reports T_g values typically in the range of 170–183 °C [60,61] for dry linear polymer; however, the thermal behaviour of poly(carboxylic acids) is known to be strongly affected by residual moisture and overlapping dehydration processes. In the present study, the DSC thermogram of PMAA exhibits a high-temperature transition in the region of 220–230 °C (Fig. 6B), which corresponds to the glass-transition region accompanied by dehydration and partial anhydride formation typical for poly(methacrylic acid). The IPC samples exhibit a single glass transition temperature in the range of 105–117 °C, located between the T_g values of the individual components but significantly higher than those of the poly(2-oxazolines). The appearance of a single T_g indicates the formation of homogeneous amorphous phases at the molecular level. The shift of T_g to higher temperatures compared with the individual poly (2-oxazolines) reflects restricted segmental mobility caused by intermolecular hydrogen bonding between the amide groups of poly (2-oxazolines) and the carboxylic groups of PMAA. Thus, the DSC results provide additional evidence for the formation of hydrogen-bonded interpolymer complexes in these systems.

3.3. *Quantum-chemical studies of the nature of hydrogen bonding in IPCs*

The presence of two potential proton-accepting sites in poly(2-oxazolines)—the nitrogen atom and the carbonyl group—raises the question of which site predominantly contributes to hydrogen bonding with the carboxylic groups of PMAA. In our previous studies, we speculated on the possible structural organisation of hydrogen bonds in IPCs of poly(2-oxazolines), involving either the nitrogen atom [39] or the carbonyl group [41], but no experimental investigations were carried out to determine the actual bonding arrangement.

In the present study, geometry optimisations and electronic structure calculations of hydrogen bonding in the interpolymer complexes were carried out using the quantum-chemical DFTB method with 3ob-3-1 parameters and the Grimme D3(BJ) dispersion correction.

When performing these calculations, it is important to account for the fact that PMAA can exist in several configurations. One such configuration is syndiotactic, in which the –COOH side groups alternate sides along the polymer backbone (see Fig. 7, schemes a and b). Another is the isotactic configuration, where all carboxyl groups are oriented in the same direction (see Fig. 7, schemes c and d).

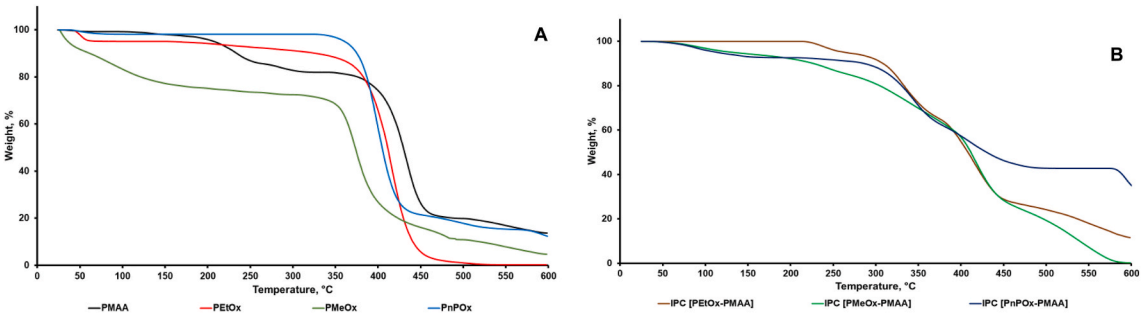

Fig. 5. TGA thermograms of individual polymers (A) and their IPCs (B).

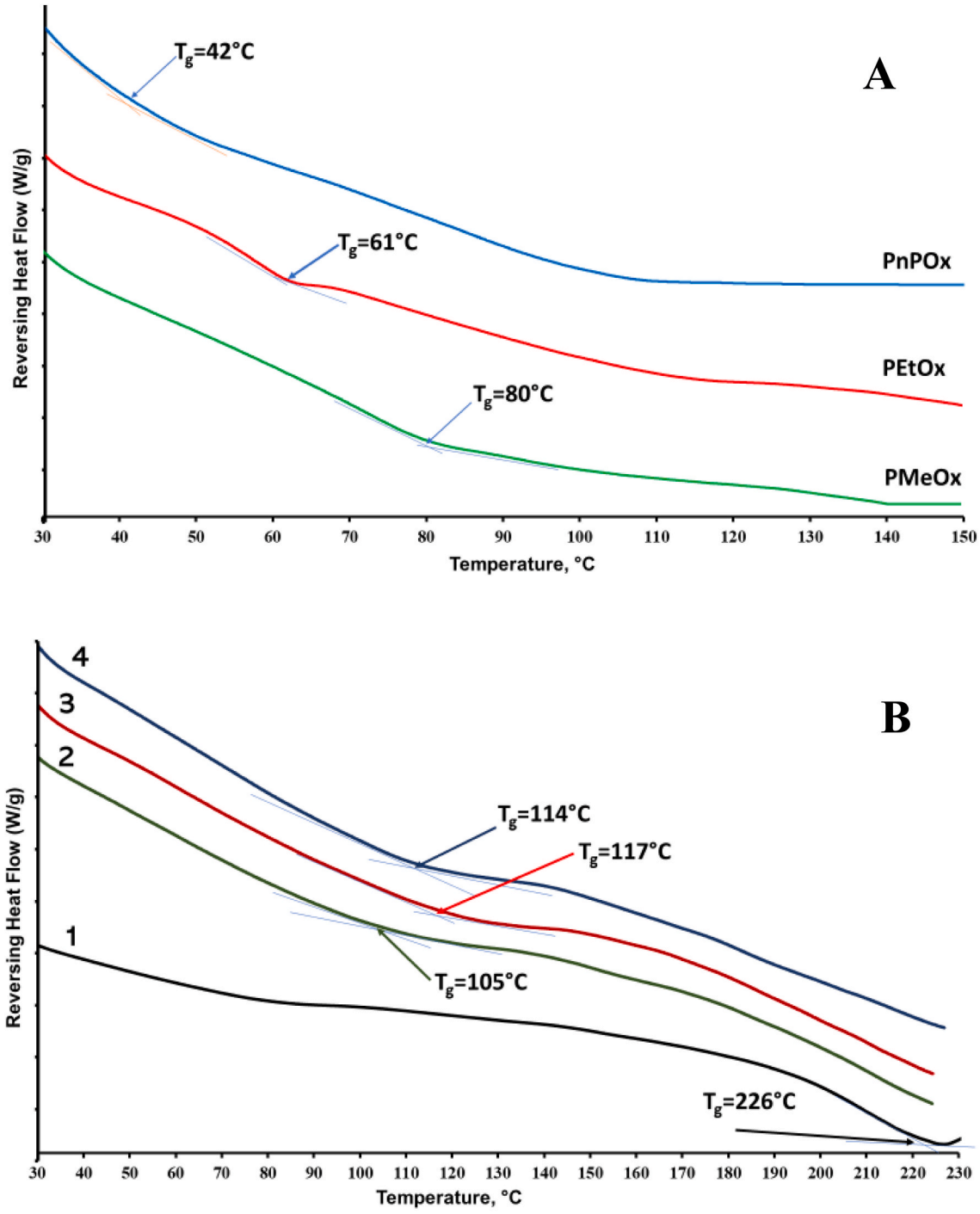

1 – PMAA; 2 - IPC [PMeOx –PMAA]; 3 - IPC [PEtOx –PMAA]; 4 - IPC [PnPOx – PMAA].

Fig. 6. DSC thermograms of individual poly(2-alkyl-2-oxazolines) (A) and PMAA and the corresponding interpolymer complexes [PMeOx–PMAA], [PEtOx–PMAA], and [PnPOx–PMAA] (B).

In the modelling of IPCs, various initial geometries were constructed by coordinating PMeOx with PMAA in different orientations to explore all plausible hydrogen bonding interactions between their functional groups. As shown in Fig. 8a and c, the initial configurations allowed for hydrogen bond formation between the carboxyl group of PMAA and the nitrogen atom of PMeOx. In contrast, Fig. 8b and d depict coordination between the carboxyl group of PMAA and the carbonyl oxygen of PMeOx. Fig. 8a and b correspond to the syndiotactic configuration of PMAA, while Fig. 8c and d correspond to the isotactic configuration.

Upon geometry optimisation, the complexes initially coordinated via the carbonyl oxygen of PMeOx (Fig. 8b and d) remained stable and unchanged. However, the configurations involving coordination through the nitrogen atom of PMeOx (Fig. 8a and c) underwent structural rearrangement, with PMeOx reorienting toward the carbonyl oxygen of PMAA. A subsequent analysis of the optimisation energies of the complexes revealed that structures coordinated via amide oxygen

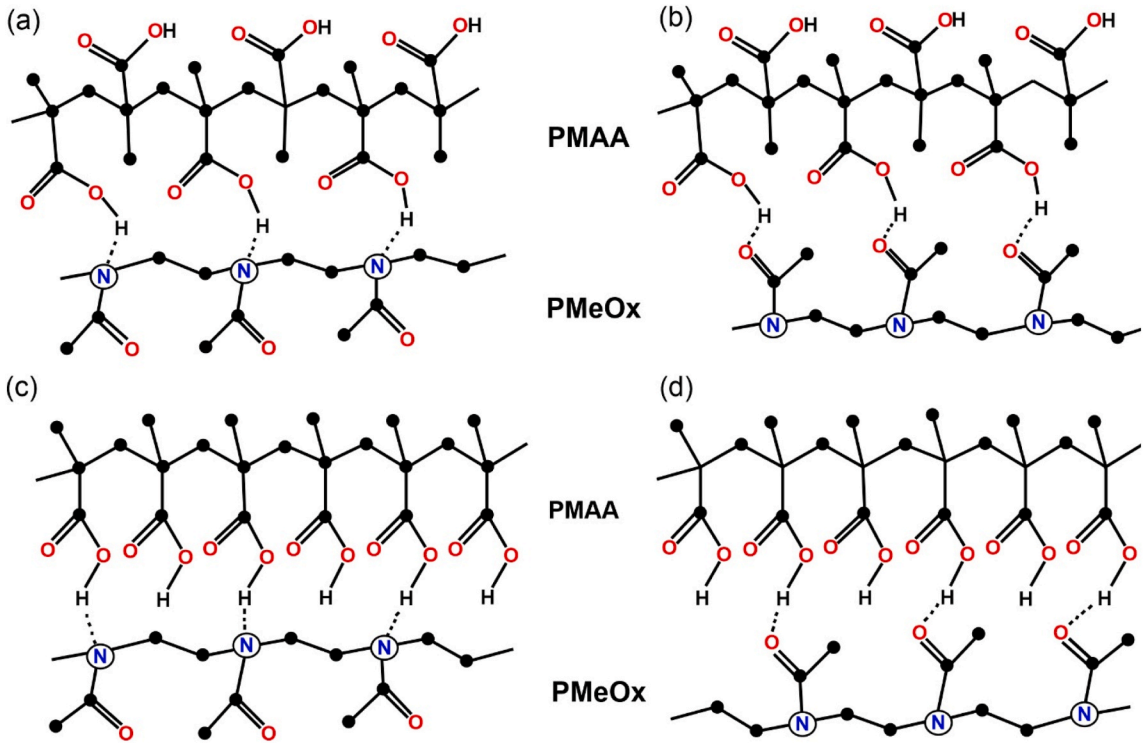

Fig. 7. Schematic representation of possible hydrogen bonding interactions in IPCs, considering different PMAA configurations. For syndiotactic PMAA, hydrogen bonds with PMeOx may form via the amide nitrogen or amide oxygen (Schemes a and b, respectively). For isotactic PMAA, similar interactions are possible, with bonding occurring through the amide nitrogen or amide oxygen (schemes c and d, respectively).

exhibit significantly lower energies (−112 and −90 kJ/mol) compared to complexes coordinated via amide nitrogen (−50 and −70 kJ/mol). This finding suggests an enhanced thermodynamic stability of the latter. This behaviour indicates a more energetically favourable interaction through the carbonyl oxygen, highlighting its dominant role in hydrogen bonding within the IPC structure.

The IPC model and the results of its geometry optimisation are presented in Fig. 8a–d. According to the calculations, the most energetically favourable structures are those in which the greatest number of hydrogen bonds are formed between PMAA and PMeOx (Fig. 8b and d). A comparison of the calculated and experimental IR spectra of syndiotactic and isotactic configurations of PMAA demonstrated a favourable agreement of frequencies in several regions of both conformations (531–581, 1129–1201, 1650–1774, 2922–3031, 3450–3645 cm^{-1}). Concurrently, the experimental spectrum displays pronounced peaks within the 1421-1441 cm^{-1} region, which are conspicuously absent in theoretical models. These peaks are consistent with the deformation vibrations of $–CH_3$ groups in proximity to carbonyl groups. The pronounced intensity of the peaks observed in the experimental spectrum, in contrast to the calculated spectra, can be attributed to the substantial concentration of these groups within the actual polymer. This discrepancy can be attributed to the limitations of the shortened model employed, which does not account for their combined contribution. In addition, calculations comparing the syndiotactic and isotactic configurations of PMAA revealed that the syndiotactic configuration is energetically more favourable by 77 kJ/mol. The theoretical spectrum of isotactic PMAA shows a shoulder at 1741 cm^{-1}, which is absent in the experimental spectrum. Moreover, the characteristic bands associated with the isotactic configuration exhibit greater intensity than observed experimentally (Fig. 9). Taken together, these spectral and energetic data suggest that PMAA predominantly adopts the syndiotactic configuration under the conditions studied.

Consequently, the structural model shown in Fig. 8b was selected for vibrational spectrum calculations and subsequently compared with experimental data. The calculated and experimental IR spectra of PMAA, PMeOx, and their interpolymer complex are presented in the Supporting Information (Fig. S11).

The most intense peak in the IR spectrum of PMAA appears at 1747 cm^{-1} and corresponds to the stretching vibrations of the C═O groups in the carboxylic acid moieties (Fig. 10).

In the 1129–1137 cm^{-1} region, deformation vibrations of the $–CH_3$ and $–CH_2$ groups of PMAA are observed, reflecting the flexibility of the polymer backbone. The 1654–1680 cm^{-1} range corresponds to the stretching vibrations of the C═O carbonyl groups in PMeOx, with one peak exhibiting high intensity, consistent with the experimental spectrum. The 1510–1523 cm^{-1} region involves a combination of C═N stretching and $–CH_2$ deformation vibrations from PMeOx units.

In the IR spectrum of the IPC, two distinct peaks are observed, indicative of interactions between PMAA and PMeOx fragments (Fig. 10). Vibrational bands at 1684 and 1745/1746 cm^{-1} are attributed to the stretching vibrations of the C═O groups in PMAA, while peaks at 1665 and 1668 cm^{-1} represent the combined contributions of C═O stretching from both PMAA and PMeOx. Additionally, the presence of an intense signal in the 3021–3065 cm^{-1} region supports the formation of hydrogen bonds between PMAA and PMeOx. As shown in Fig. 10, the calculated vibrational frequencies exhibit good agreement with the experimental IR spectra.

These findings collectively confirm that PMAA forms stable and distinct IPCs with PEtOx, PMeOx, and PnPOx, characterised by specific hydrogen bonding interactions and structural rearrangements that are not present in the individual polymers.

3.4. Molecular iodine absorption by individual polymers and their IPCs in the solid state

Many water-soluble polymers are known to form complexes with molecular iodine, and such complexes are commonly used as antiseptic agents [62,63]. In addition to these applications, molecular iodine can

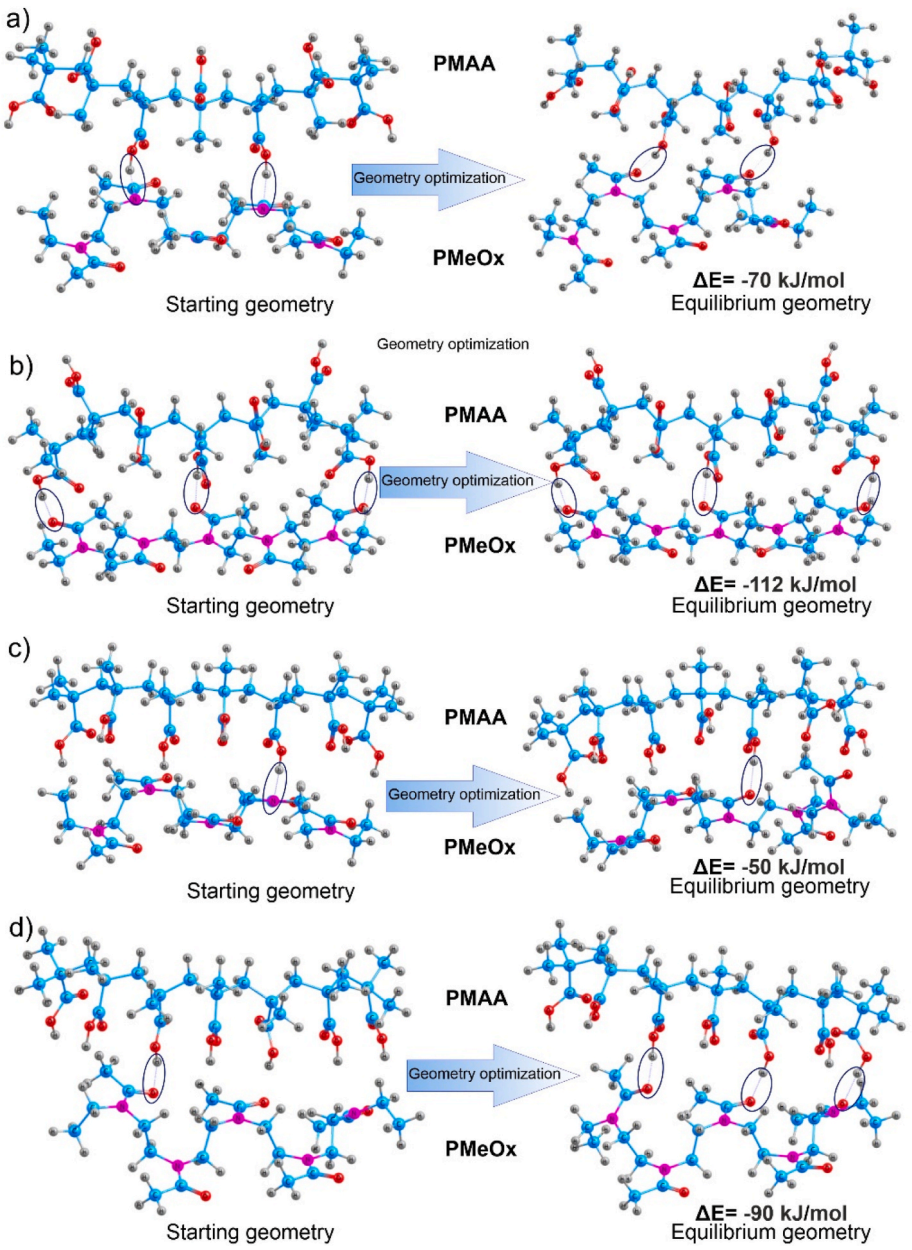

Fig. 8. Initial models and geometry-optimised structures of IPCs formed between PMAA and PMeOx. a, b – syndiotactic configuration of PMAA; c, d – isotactic configuration of PMAA. ΔE indicates the formation energy of the IPC.

be used as a sensitive molecular probe for investigating the microenvironment and accessibility of functional groups in polymer systems. In our previous work [40] we demonstrated that poly(2-ethyl-2-oxazoline) forms iodine complexes in solution and exhibits a stronger iodine-binding capacity than poly(N-vinylpyrrolidone). In the present study, the absorption of iodine vapours was investigated using the dry forms of the individual polymers and their corresponding IPCs, using iodine as a molecular probe to assess changes in functional group accessibility in the solid state.

During exposure to iodine vapours, the samples exhibited noticeable colour changes ranging from yellow to dark brown or black, depending on the polymer. Photographs of the initial polymers and the corresponding IPCs after iodine treatment are shown in Fig. 11. Following iodine absorption, the samples exhibited distinct differences in colour and morphology. PMAA remained as yellowish granules, while PMeOx and PEtOx developed bluish hues. PnPOx displayed a dark, clustered appearance. The IPCs formed fine powders with colours ranging from light brown to dark brown, depending on the specific polymer combination. To determine the extent of iodine vapour absorption by the dry polymer and IPC samples, the samples were dissolved in ethanol, and the iodine content in the resulting solutions was quantified spectrophotometrically at 444 nm.

The degree of iodine absorption varied significantly among the initial polymers and IPCs (Fig. 11). Among the individual polymers, PEtOx and PnPOx exhibited the highest absorption capacities, at approximately 25.15% and 22.98%, respectively. In contrast, PMeOx showed a markedly lower sorption level (~10.78%), while PMAA demonstrated minimal iodine uptake (0.53%), reflecting its limited interaction with iodine vapours under the experimental conditions. Statistical analysis revealed highly significant differences in iodine sorption between PMAA and each of the poly(2-oxazoline) polymers: PEtOx and PnPOx ($p < 0.0001$), and PMeOx ($p < 0.001$). Additionally, PnPOx and PEtOx exhibited significantly greater absorption than PMeOx ($p < 0.01$ and $p < 0.001$, respectively), highlighting the

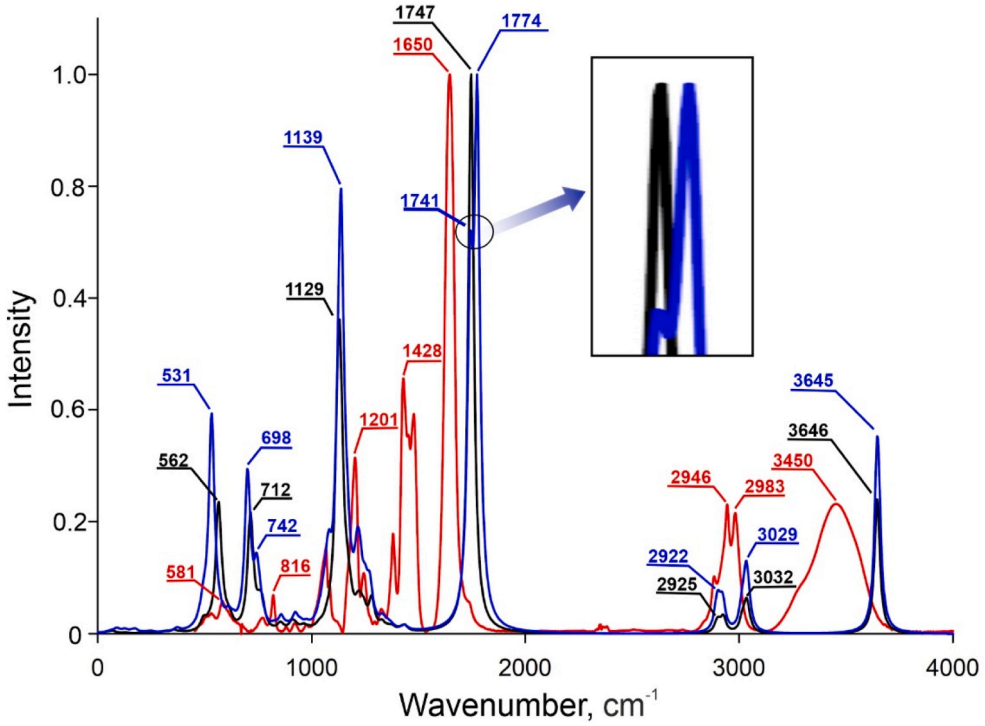

Fig. 9. Comparison of experimental and theoretical infrared (IR) spectra of PMAA in isotactic and syndiotactic configurations. Red – experimental spectrum; black – theoretical spectrum for the syndiotactic conformation; blue – theoretical spectrum for the isotactic configuration. (For interpretation of the references to colour in this figure legend, the reader is referred to the Web version of this article.)

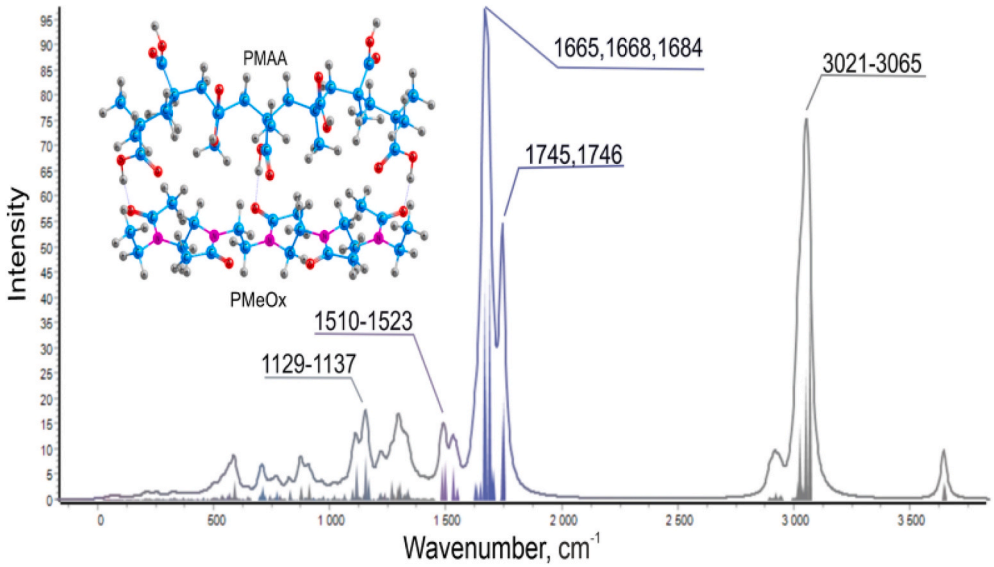

Fig. 10. Calculated IR spectrum of the IPC. Line colours indicate the types of atoms primarily involved in the vibrational modes within the IPC structure. (For interpretation of the references to colour in this figure legend, the reader is referred to the Web version of this article.)

influence of poly(2-oxazoline) structure on iodine affinity. In contrast, the IPC samples exhibited substantially reduced iodine absorption, with values of 2.81%, 0.63%, and 4.74%, respectively.

Since all samples were analysed as dry, finely dispersed powders of identical mass and exposed to iodine vapour under identical conditions, the observed differences in iodine uptake can be attributed primarily to differences in the accessibility of iodine-binding functional groups rather than to macroscopic variations in sample morphology. Under these conditions, iodine molecules can gradually diffuse into the bulk of the polymer samples, enabling interaction with accessible functional groups and subsequent complex formation.

The decrease in iodine sorption upon complex formation can be explained by the formation of a compact hydrogen-bonded network between PMAA and poly(2-oxazolines). These interactions restrict the accessibility of the amide carbonyl groups of poly(2-oxazolines), which are known to act as the main iodine-binding sites. As a result, the free poly(2-oxazolines) exhibit significantly higher iodine uptake compared to their corresponding interpolymer complexes.

These results demonstrate that iodine vapour sorption can serve as a convenient probe for assessing structural compaction and functional

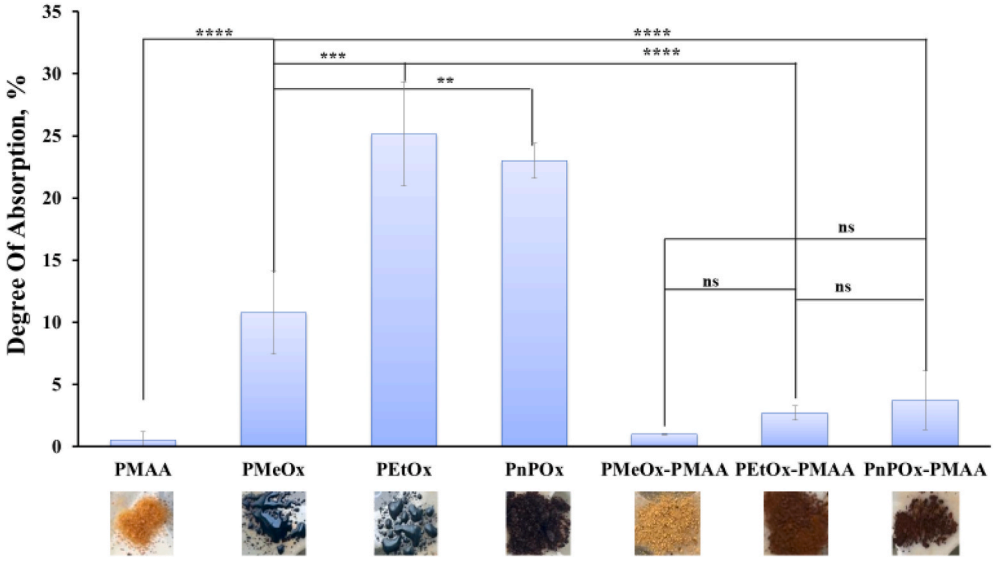

Fig. 11. Comparative analysis of iodine absorption by initial polymers (PMAA, PMeOx, PEtOx, PnPOx) and their IPCs. Statistical significance is indicated as follows: **** - $p < 0.0001$; *** - $p < 0.001$; ** - $p < 0.01$ and no statistically significant difference – $p > 0.05$.

group accessibility in hydrogen-bonded interpolymer complexes.

4. Conclusions

The formation of hydrogen-bonded complexes between poly(methacrylic acid) (PMAA) and three poly(2-alkyl-2-oxazolines) was investigated in aqueous solutions across a range of pH values and polymer concentrations. The critical pH values for complexation were determined using turbidimetry, viscometry, and dynamic light scattering. These measurements indicate that all three poly(2-alkyl-2-oxazolines) form strong hydrogen-bonded complexes with PMAA, with complexation strength increasing from the methyl to ethyl to n-propyl derivatives. This trend suggests that hydrophobic interactions contribute additional stabilisation to the interpolymer complexes.

In the solid state, the interpolymer complexes exhibit thermal properties distinct from those of the individual polymers, including a single glass transition temperature (T_g) that is higher than the T_g values of the individual components. This behaviour is attributed to the formation of a strong network of intermacromolecular hydrogen bonds, which restricts segmental mobility within the complex.

Quantum-chemical calculations revealed that the most energetically favourable hydrogen bond within the interpolymer complexes involves the carbonyl oxygen of poly(2-alkyl-2-oxazoline) forming a hydrogen bond with the proton of the undissociated carboxylic acid group (–COOH) in poly(methacrylic acid).

In the dry state, poly(2-alkyl-2-oxazolines) demonstrated a strong ability to bind iodine from the vapour phase, whereas poly(methacrylic acid) alone did not exhibit this property. However, complexation with poly(methacrylic acid) significantly reduced the iodine-binding capacity of poly(2-alkyl-2-oxazolines), likely due to the blocking of reactive sites involved in iodine absorption.

Studies on interpolymer complexes suggest that these materials may be useful in applications requiring pH-responsive solubility and moisture-triggered release. Potential application areas include drug delivery, agrochemical formulations, and other controlled-release technologies. In view of the poor binding of molecular iodine by the interpolymer complexes, these materials are not suitable as carriers for this antimicrobial agent. In contrast, individual poly(2-oxazolines) may be considered promising candidates for this application because of their strong affinity for iodine.

CRediT authorship contribution statement

Danelya N. Makhayeva: Writing – original draft, Visualization, Resources, Methodology, Investigation, Funding acquisition, Formal analysis, Data curation. **Dilnaz A. Tolegenova:** Methodology, Investigation. **Adina M. Abiyeva:** Investigation. **Galiya S. Irmukhametova:** Writing – review & editing, Supervision, Project administration, Methodology, Funding acquisition. **Grigoriy A. Mun:** Supervision, Methodology, Funding acquisition. **Ruslan Y. Smyslov:** Writing – review & editing, Validation, Resources, Methodology, Formal analysis. **Yulia E. Gorshkova:** Validation, Resources, Methodology, Investigation, Funding acquisition, Formal analysis, Data curation. **Vlada E. Ivanova:** Visualization, Validation, Software, Methodology, Investigation, Formal analysis, Data curation. **Felix N. Tomilin:** Visualization, Validation, Software, Resources, Methodology, Investigation, Formal analysis, Data curation. **Vitaliy V. Khutoryanskiy:** Writing – review & editing, Supervision, Resources, Project administration, Funding acquisition, Conceptualization.

Declaration of competing interest

The authors declare the following financial interests/personal relationships which may be considered as potential competing interests: Danelya Makhayeva reports financial support was provided by Ministry of Science and Higher Education of the Republic of Kazakhstan. Danelya Makhayeva, Dilnaz Tolegenova, Galiya Irmukhametova, Grigoriy Mun report financial support was provided by Committee of Science of the Ministry of Science and Higher Education of the Republic of Kazakhstan. Galiya Irmukhametova and Yuliya Gorshkova report financial support was provided by from the JINR—Republic of Kazakhstan cooperation program. Vitaliy Khutoryanskiy reports financial support was provided by The Royal Society. If there are other authors, they declare that they have no known competing financial interests or personal relationships that could have appeared to influence the work reported in this paper.

Acknowledgements

DNM acknowledges the Ministry of Science and Higher Education of the Republic of Kazakhstan for the research grant for young scientists « Zhas Galym» 2023-2025. (No. AP19176452). DNM, DTA, GSI, GAM and VVK acknowledge the Committee of Science of the Ministry of Science and Higher Education of the Republic of Kazakhstan (Grant No

BR24993113). GSI and YuEG are very grateful to the scientific project 04-4-1149-2-2021/2028, with financial support from the JINR—Republic of Kazakhstan cooperation program in 2024-2025 (Project 448 dated 06.06.2024, clause 6 and Project 36 dated 23.01.2025, clause 4). FNT and VEI carried out the quantum chemical study within the state assignment of the Kirensky Institute of Physics. RYS conducted the IPC study as part of state assignment No. 1023031700043-2-1.4.4. Additionally, VVK acknowledges the Royal Society for his Industry Fellowship (IF\R2\222031).

During the preparation of this work, the author(s) used ChatGPT (OpenAI) to assist with the clarity and flow of some parts of the manuscript. After using this tool/service, the author(s) reviewed and edited the content as needed and take(s) full responsibility for the content of the publication. The graphical abstract was designed using Chemix (https://chemix.org), with partial support from ChatGPT (OpenAI) for content generation.

Appendix A. Supplementary data

Supplementary data to this article can be found online at https://doi.org/10.1016/j.polymer.2026.130028.

Data availability

Data will be made available on request.

References

[1] E.A. Bekturov, L.A. Bimendina, Interpolymer Complexes, 1981, pp. 99–147, https://doi.org/10.1007/3-540-10554-9_11.
[2] V.A. Kabanov, Interpolymer complexes as new materials for biomedical applications, Makromol. Chem., Macromol. Symp. 48–49 (1) (1991) 425–426, https://doi.org/10.1002/masy.19910480131.
[3] E. Tsuchida, K. Abe, Interactions between macromolecules in solution and intermacromolecular complexes, Adv. Polym. Sci. 45 (1982) 1–126, https://doi.org/10.1007/BFb0017549.
[4] E. Tsuchida, Y. Osada, H. Ohno, Formation of interpolymer complexes, J. Macromol. Sci. B 17 (4) (1980) 683–714, https://doi.org/10.1080/00222348008212832.
[5] V.V. Khutoryanskiy, G. Staikos, Hydrogen-Bonded Interpolymer Complexes, WORLD SCIENTIFIC, 2009, https://doi.org/10.1142/6498.
[6] V. Kozlovskaya, E. Kharlampieva, M.L. Mansfield, S.A. Sukhishvili, Poly (Methacrylic acid) hydrogel films and capsules: response to PH and ionic strength, and encapsulation of macromolecules, Chem. Mater. 18 (2) (2006) 328–336, https://doi.org/10.1021/cm0517364.
[7] R.F. Schmidt, J. Lutzki, R. Dalgliesh, S. Prévost, M.P.H.- Gradzielski, Responsive rheology and structure of Poly(Ethylene Oxide)–Poly(Methacrylic acid) interpolymer complexes, Macromolecules 58 (1) (2025) 321–333, https://doi.org/10.1021/acs.macromol.4c02726.
[8] E. Kharlampieva, V. Kozlovskaya, J. Tyutina, S.A. Sukhishvili, Hydrogen-Bonded multilayers of thermoresponsive polymers, Macromolecules 38 (25) (2005) 10523–10531, https://doi.org/10.1021/ma0516891.
[9] A. Usaitis, S.L. Maunu, H. Tenhu, Aggregation of the interpolymer complex of Poly (Methacrylic acid) and Poly(Vinyl Pyrrolidone) in aqueous solutions, Eur. Polym. J. 33 (2) (1997) 219–223, https://doi.org/10.1016/S0014-3057(96)00125-5.
[10] V.V. Khutoryanskiy, Hydrogen-Bonded interpolymer complexes as materials for pharmaceutical applications, Int. J. Pharm. 334 (1–2) (2007) 15–26, https://doi.org/10.1016/j.ijpharm.2007.01.037.
[11] F. Zhang, J. Lubach, W. Na, S. Momin, Interpolymer complexation between polyox and carbopol, and its effect on drug release from matrix tablets, J. Pharmacol. Sci. 105 (8) (2016) 2386–2396, https://doi.org/10.1016/j.xphs.2016.05.020.
[12] Y. Chen, L. Zhang, J. Xu, S. Xu, Y. Li, R. Sun, J. Huang, J. Peng, Z. Gong, J. Wang, L. Tang, Development of a hydroxypropyl methyl Cellulose/Polyacrylic acid interpolymer complex formulated buccal mucosa adhesive film to facilitate the delivery of insulin for diabetes treatment, Int. J. Biol. Macromol. 269 (2024) 131876, https://doi.org/10.1016/j.ijbiomac.2024.131876.
[13] M.-K. Chun, C.-S. Cho, H.-K. Choi, Mucoadhesive drug carrier based on interpolymer complex of Poly(Vinyl Pyrrolidone) and Poly(Acrylic acid) prepared by template polymerization, J. Contr. Release 81 (3) (2002) 327–334, https://doi.org/10.1016/S0168-3659(02)00078-0.
[14] S. Das, M.T. Joseph, D. Sarkar, Hydrogen bonding interpolymer complex Formation and study of its host–guest interaction with Cyclodextrin and its application as an active delivery vehicle, Langmuir 29 (6) (2013) 1818–1830, https://doi.org/10.1021/la304466z.
[15] S.C. Bizley, A.C. Williams, V.V. Khutoryanskiy, Thermodynamic and kinetic properties of interpolymer complexes assessed by isothermal titration calorimetry and surface plasmon resonance, Soft Matter 10 (41) (2014) 8254–8260, https://doi.org/10.1039/C4SM01138D.
[16] M.T. Garay, C. Alava, M. Rodriguez, Study of polymer–polymer complexes and blends of Poly(N-Isopropylacrylamide) with Poly(Carboxylic acid). 2. Poly(Acrylic acid) and Poly(Methacrylic acid) partially neutralized, Polymer (Guildf). 41 (15) (2000) 5799–5807, https://doi.org/10.1016/S0032-3861(99)00765-X.
[17] D.J. Hemker, V. Garza, C.W. Frank, Complexation of Poly(Acrylic acid) and Poly (Methacrylic acid) with pyrene-end-labeled Poly(Ethylene glycol): PH and fluorescence measurements, Macromolecules 23 (20) (1990) 4411–4418, https://doi.org/10.1021/ma00222a014.
[18] T. Ikawa, K. Abe, K. Honda, E. Tsuchida, Interpolymer complex between Poly (Ethylene oxide) and Poly(Carboxylic acid), J. Polym. Sci., Polym. Chem. Ed. 13 (7) (1975) 1505–1514, https://doi.org/10.1002/pol.1975.170130703.
[19] M. Koussathana, P. Lianos, G. Staikos, Investigation of hydrophobic interactions in dilute aqueous solutions of hydrogen-bonding interpolymer complexes by steady-state and time-resolved fluorescence measurements, Macromolecules 30 (25) (1997) 7798–7802, https://doi.org/10.1021/ma9706485.
[20] G.A. Mun, Z.S. Nurkeeva, V.V. Khutoryanskiy, A.B. Bitekenova, Effect of copolymer composition on interpolymer complex formation of (Co)Poly(Vinyl Ether)s with Poly(Acrylic acid) in aqueous and organic solutions, Macromol. Rapid Commun. 21 (7) (2000) 381–384, https://doi.org/10.1002/(SICI)1521-3927(20000401)21:7<381::AID-MARC381>3.0.CO;2-B.
[21] R. Hoogenboom, Poly(2-oxazoline)s: a polymer class with numerous potential applications, Angew. Chem. Int. Ed. 48 (43) (2009) 7978–7994, https://doi.org/10.1002/anie.200901607.
[22] O. Sedlacek, B.D. Monnery, S.K. Filippov, R. Hoogenboom, M. Hruby, Poly(2-Oxazoline)s – are they more advantageous for biomedical applications than other polymers? Macromol. Rapid Commun. 33 (19) (2012) 1648–1662, https://doi.org/10.1002/marc.201200453.
[23] B. Verbraeken, B.D. Monnery, K. Lava, R. Hoogenboom, The chemistry of Poly(2-Oxazoline)s, Eur. Polym. J. 88 (2017) 451–469, https://doi.org/10.1016/j.eurpolymj.2016.11.016.
[24] R. Luxenhofer, Y. Han, A. Schulz, J. Tong, Z. He, A.V. Kabanov, R. Jordan, Poly(2-oxazoline)s as polymer therapeutics, Macromol. Rapid Commun. 33 (19) (2012) 1613–1631, https://doi.org/10.1002/marc.201200354.
[25] J. Becelaere, E. Van Den Broeck, E. Schoolaert, V. Vanhoorne, J.F.R. Van Guyse, M. Vergaelen, S. Borgmans, K. Creemers, V. Van Speybroeck, C. Vervaet, R. Hoogenboom, K. De Clerck, Stable amorphous solid dispersion of flubendazole with high loading via electrospinning, J. Contr. Release 351 (2022) 123–136, https://doi.org/10.1016/j.jconrel.2022.09.028.
[26] X. Shan, A.C. Williams, V.V. Khutoryanskiy, Polymer structure and property effects on solid dispersions with Haloperidol: poly(n-vinyl Pyrrolidone) and Poly(2-Oxazolines) studies, Int. J. Pharm. 590 (2020) 119884, https://doi.org/10.1016/j.ijpharm.2020.119884.
[27] H. Fael, C. Ràfols, A.L. Demirel, Poly(2-Ethyl-2-Oxazoline) as an alternative to Poly (Vinylpyrrolidone) in solid dispersions for solubility and dissolution rate enhancement of drugs, J. Pharmacol. Sci. 107 (9) (2018) 2428–2438, https://doi.org/10.1016/j.xphs.2018.05.015.
[28] R. Vanhoeijen, I.A. Okkelman, N. Rogier, T. Sedlačík, D.D. Stöbener, B. Devriendt, R.I. Dmitriev, R. Hoogenboom, Poly(2-Alkyl-2-Oxazoline) hydrogels as synthetic matrices for multicellular spheroid and intestinal organoid cultures, Biomacromolecules 26 (3) (2025) 1860–1872, https://doi.org/10.1021/acs.biomac.4c01627.
[29] B. Stubbe, Y. Li, M. Vergaelen, S. Van Vlierberghe, P. Dubruel, K. De Clerck, R. Hoogenboom, Aqueous electrospinning of Poly(2-Ethyl-2-Oxazoline): mapping the parameter space, Eur. Polym. J. 88 (2017) 724–732, https://doi.org/10.1016/j.eurpolymj.2016.09.014.
[30] L. Simon, V. Lapinte, L. Lionnard, N. Marcotte, M. Morille, A. Aouacheria, K. Kissa, J.M. Devoisselle, S. Bégu, Polyoxazolines based lipid nanocapsules for topical delivery of antioxidants, Int. J. Pharm. 579 (2020) 119126, https://doi.org/10.1016/j.ijpharm.2020.119126.
[31] D. Hwang, T. Dismuke, A. Tikunov, E.P. Rosen, J.R. Kagel, J.D. Ramsey, C. Lim, W. Zamboni, A.V. Kabanov, T.R. Gershon, M. Sokolsky-Papkov PhD, Poly(2-Oxazoline) nanoparticle delivery enhances the therapeutic potential of vismodegib for medulloblastoma by improving CNS pharmacokinetics and reducing systemic toxicity, Nanomedicine 32 (2021) 102345, https://doi.org/10.1016/j.nano.2020.102345.
[32] A.L. Onugwu, A.A. Attama, P.O. Nnamani, S.O. Onugwu, E.B. Onuigbo, V. V. Khutoryanskiy, Development and optimization of solid lipid nanoparticles coated with Chitosan and Poly(2-Ethyl-2-Oxazoline) for ocular drug delivery of ciprofloxacin, J. Drug Deliv. Sci. Technol. 74 (2022) 103527, https://doi.org/10.1016/j.jddst.2022.103527.
[33] G.K. Abilova, S.F. Nasibullin, K. Ilyassov, A.N. Adilov, M.K. Akhmetova, R. I. Moustafine, Y.T. Muratov, S.E. Kudaibergenov, V.V. Khutoryanskiy, Mucoadhesive gellan Gum/Poly(2-Ethyl-2-Oxazoline) films for ocular delivery of pilocarpine hydrochloride, J. Drug Deliv. Sci. Technol. 104 (2025) 106492, https://doi.org/10.1016/j.jddst.2024.106492.
[34] E.M. Chistyakov, S.N. Filatov, E.A. Sulyanova, V.V. Volkov, Determination of the degree of crystallinity of Poly(2-Methyl-2-Oxazoline), Polymers 13 (24) (2021) 4356, https://doi.org/10.3390/polym13244356.
[35] N. Oleszko-Torbus, A. Utrata-Wesołek, M. Bochenek, D. Lipowska-Kur, A. Dworak, W. Wałach, Thermal and crystalline properties of Poly(2-Oxazoline)s, Polym. Chem. 11 (1) (2020) 15–33, https://doi.org/10.1039/C9PY01316D.
[36] E. Cagli, E. Ugur, S. Ulusan, S. Banerjee, I. Erel-Goktepe, Effect of side chain variation on surface and biological properties of Poly(2-Alkyl-2-Oxazoline)

multilayers, Eur. Polym. J. 114 (2019) 452–463, https://doi.org/10.1016/j.eurpolymj.2019.02.031.
[37] T.N. Nekrasova, T. Yu Kirila, M.P. Kurlykin, A.V. Ten'kovtsev, A.P. Filippov, Interpolymer complexes of star-shaped copolymers of polyoxazoline with the calixarene core and Linear polyacids in solution, Polym. Sci. B 63 (2) (2021) 116–125, https://doi.org/10.1134/S1560090421020081.
[38] J. Dai, S.H. Goh, S.Y. Lee, K.S. Siow, Miscibility and interpolymer complexation of Poly(2-Methyl-2-Oxazoline) with hydroxyl-containing polymers, J. Polym. Res. 2 (4) (1995) 209–215, https://doi.org/10.1007/BF01492772.
[39] R.I. Moustafine, A.S. Viktorova, V.V. Khutoryanskiy, Interpolymer complexes of carbopol® 971 and Poly(2-Ethyl-2-Oxazoline): physicochemical studies of complexation and formulations for oral drug delivery, Int. J. Pharm. 558 (2019) 53–62, https://doi.org/10.1016/j.ijpharm.2019.01.002.
[40] D.N. Makhayeva, S.K. Filippov, S.S. Yestemes, G.S. Irmukhametova, V. V. Khutoryanskiy, Polymeric iodophors with Poly(2-Ethyl-2-Oxazoline) and Poly (N-Vinylpyrrolidone): optical, hydrodynamic, thermodynamic, and antimicrobial properties, Eur. Polym. J. 165 (2022) 111005, https://doi.org/10.1016/j.eurpolymj.2022.111005.
[41] R.Y. Smyslov, Y.E. Gorshkova, T.N. Nekrasova, D.N. Makhayeva, G.A. Mun, G. S. Irmukhametova, V.V. Khutoryanskiy, Dynamic and structural insights into hydrogen-bonded interpolymer complexes of Poly(2-Alkyl-2-Oxazolines) with Poly (Carboxylic acids), J. Colloid Interface Sci. (2025) 138185, https://doi.org/10.1016/j.jcis.2025.138185.
[42] Z.S. Nurkeeva, G.A. Mun, V.V. Khutoryanskiy, A.A. Zotov, R.A. Mangazbaeva, Interpolymer complexes of Poly(Vinyl ether) of ethylene glycol with Poly (Carboxylic acids) in aqueous, alcohol and mixed solutions, Polymer (Guildf). 41 (21) (2000) 7647–7651, https://doi.org/10.1016/S0032-3861(00)00143-9.
[43] M. Gaus, A. Goez, M. Elstner, Parametrization and benchmark of DFTB3 for organic molecules, J. Chem. Theor. Comput. 9 (1) (2013) 338–354, https://doi.org/10.1021/ct300849w.
[44] A.V. Marenich, C.J. Cramer, D.G. Truhlar, Universal solvation model based on Solute electron density and on a continuum model of the solvent defined by the bulk dielectric constant and atomic surface tensions, J. Phys. Chem. B 113 (18) (2009) 6378–6396, https://doi.org/10.1021/jp810292n.
[45] G.M.J. Barca, C. Bertoni, L. Carrington, D. Datta, N. De Silva, J.E. Deustua, D. G. Fedorov, J.R. Gour, A.O. Gunina, E. Guidez, T. Harville, S. Irle, J. Ivanic, K. Kowalski, S.S. Leang, H. Li, W. Li, J.J. Lutz, I. Magoulas, J. Mato, V. Mironov, H. Nakata, B.Q. Pham, P. Piecuch, D. Poole, S.R. Pruitt, A.P. Rendell, L.B. Roskop, K. Ruedenberg, T. Sattasathuchana, M.W. Schmidt, J. Shen, L. Slipchenko, M. Sosonkina, V. Sundriyal, A. Tiwari, J.L. Galvez Vallejo, B. Westheimer, M. Włoch, P. Xu, F. Zahariev, M.S. Gordon, Recent developments in the general atomic and molecular electronic structure System, J. Chem. Phys. 152 (15) (2020), https://doi.org/10.1063/5.0005188.
[46] O. Aviv, N. Laout, S. Ratner, O. Harik, K.R. Kunduru, A.J. Domb, Controlled iodine release from polyurethane sponges for water decontamination, J. Contr. Release 172 (3) (2013) 634–640.
[47] V.V. Khutoryanskiy, G.A. Mun, Z.S. Nurkeeva, A.V. Dubolazov, PH and salt effects on interpolymer complexation via hydrogen bonding in aqueous solutions, Polym. Int. 53 (9) (2004) 1382–1387, https://doi.org/10.1002/pi.1549.
[48] Z.S. Nurkeeva, G.A. Mun, V.V. Khutoryanskiy, Interpolymer complexes of Poly (Glycol vinyl ethers) and related composite materials, Polym. Sci. B 43 (5–6) (2001) 148–157.
[49] S.K. Filippov, R. Khusnutdinov, A. Murmiliuk, W. Inam, L. Ya Zakharova, H. Zhang, V.V. Khutoryanskiy, Dynamic light scattering and transmission electron microscopy in drug delivery: a roadmap for correct characterization of nanoparticles and interpretation of results, Mater. Horiz. 10 (12) (2023) 5354–5370, https://doi.org/10.1039/D3MH00717K.
[50] Z.S. Nurkeeva, G.A. Mun, V.V. Khutoryanskiy, A.D. Sergaziev, Complex Formation between Poly(Vinyl ether of diethyleneglycol) and polyacrylic acid, Eur. Polym. J. 37 (6) (2001) 1233–1237, https://doi.org/10.1016/S0014-3057(00)00237-8.
[51] G.A. Mun, Z.S. Nurkeeva, V.V. Khutoryanskiy, G.S. Sarybayeva, A.V. Dubolazov, PH-Effects in the complex Formation of Polymers I. Interaction of Poly(Acrylic acid) with Poly(Acrylamide), Eur. Polym. J. 39 (8) (2003) 1687–1691, https://doi.org/10.1016/S0014-3057(03)00065-X.
[52] Z.S. Nurkeeva, G.A. Mun, V.V. Khutoryanskiy, A.B. Bitekenova, A.V. Dubolazov, S. Z. Esirkegenova, PH effects in the Formation of interpolymer complexes between Poly(N-Vinylpyrrolidone) and Poly(Acrylic acid) in aqueous solutions, Euro Phys.J. E 10 (1) (2003) 65–68, https://doi.org/10.1140/epje/e2003-00003-4.
[53] A.M. Lichkus, P.C. Painter, M.M. Coleman, Hydrogen bonding in polymer blends. 5. Blends involving polymers containing methacrylic acid and oxazoline groups, Macromolecules 21 (8) (1988) 2636–2641, https://doi.org/10.1021/ma00186a054.
[54] Y. Matsuda, K. Takatsuji, Y. Shiokawa, M. Kikuchi, S. Kidoaki, A. Takahara, S. Tasaka, Characterization of complexes formed by mixing aqueous solutions of Poly(2-Ethyl-2-Oxazoline) and Poly(Methacrylic acid) with a wide range of concentrations, Polymer (Guildf). 54 (7) (2013) 1896–1904, https://doi.org/10.1016/j.polymer.2013.02.004.
[55] H.G. Schild, Thermal degradation of Poly(Methacrylic acid): further studies applying TGA/FTIR, J. Polym. Sci. Polym. Chem. 31 (9) (1993) 2403–2405, https://doi.org/10.1002/pola.1993.080310925.
[56] P. Bouten, K. Lava, J. Van Hest, R. Hoogenboom, Thermal properties of methyl ester-containing Poly(2-Oxazoline)s, Polymers 7 (10) (2015) 1998–2008, https://doi.org/10.3390/polym7101494.
[57] H.M.L. Lambermont-Thijs, L. Bonami, F.E. Du Prez, R. Hoogenboom, Linear Poly (Alkyl ethylene imine) with varying side chain length: synthesis and physical properties, Polym. Chem. 1 (5) (2010) 747, https://doi.org/10.1039/b9py00344d.
[58] T. Konings, B. Goderis, R. Hoogenboom, W. Marchal, G. Van den Mooter, Unraveling the physicochemical properties of Poly(2- n -Propyl-2-Oxazoline), a promising pharmaceutical excipient, Macromolecules 58 (16) (2025) 8727–8740, https://doi.org/10.1021/acs.macromol.5c00794.
[59] A. Samaro, M. Vergaelen, M. Purino, A. Tigrine, V.R. de la Rosa, N.M. Goudarzi, M. N. Boone, V. Vanhoorne, R. Hoogenboom, C. Vervaet, Poly(2-Alkyl-2-Oxazoline)s: a polymer platform to sustain the release from tablets with a high drug loading, Mater. Today Bio 16 (2022) 100414, https://doi.org/10.1016/j.mtbio.2022.100414.
[60] V.F. Ur'yash, N. Yu Kokurina, V.N. Larina, S.V. Chuprova, Thermodynamic characteristics and the temperatures of relaxation transitions of Poly(Methacrylic acid), Polym. Sci. 56 (1) (2014) 32–39, https://doi.org/10.1134/S0965545X14010118.
[61] C.-F. Huang, F.-C. Chang, Comparison of hydrogen bonding interaction between PMMA/PMAA blends and PMMA-Co-PMAA copolymers, Polymer (Guildf). 44 (10) (2003) 2965–2974, https://doi.org/10.1016/S0032-3861(03)00188-5.
[62] D.N. Makhayeva, G.S. Irmukhametova, V.V. Khutoryanskiy, Polymeric iodophors: preparation, properties, and biomedical applications, Rev. J. Chem. 10 (1) (2020) 40–57, https://doi.org/10.1134/S2079978020010033.
[63] D.N. Makhayeva, G.S. Irmukhametova, V.V. Khutoryanskiy, Advances in antimicrobial polymeric iodophors, Eur. Polym. J. 201 (2023) 112573, https://doi.org/10.1016/j.eurpolymj.2023.112573.